ACI STRUCTURAL JOURNAL TECHNICAL PAPER

Title no. 100-S81

Retrofit of Square Concrete Columns with Carbon Fiber-Reinforced Polymer for Seismic Resistance

by Richard D. Iacobucci, Shamim A. Sheikh, and Oguzhan Bayrak

Reinforced concrete columns lacking sufficient lateral steel do not possess the necessary ductility to dissipate seismic energy during a major earthquake without severe strength degradation. This paper investigates the prospect of strengthening deficient and repairing damaged square columns with carbon fiber-reinforced polymer (CFRP) jackets. Eight specimens representative of members in buildings and bridges constructed before 1971 consisted of a 305 x 305 x 1473 mm column connected to a 508 x 762 x 813 mm stub. Each 900 kg specimen was tested under lateral cyclic displacement excursions and simultaneous constant axial load to simulate seismic forces. Results indicate that added confinement with CFRP at critical locations enhanced ductility, energy dissipation capacity, and strength of all substandard members. A positive relationship prevailed between favorable behavior and increasing reinforcement layers while improvements realized through CFRP repair declined as damage level prior to retrofit increased. Appropriately strengthened specimens also exceeded the performance of comparable columns with adequate seismic lateral reinforcement.

Keywords: columns; concrete; ductility; fibers; repair.

INTRODUCTION

Large inelastic deformation limits of individual members allow entire structures to endure severe ground motion while dissipating significant levels of seismic energy. Plastic hinge formation associated with lateral displacement excursions is favored in beams and girders rather than in columns to ensure that overall structural integrity is not compromised. Plastic hinge development can occur in columns, however, particularly at the bases of multistory frames and bridges where incurred damage acts to dampen seismic forces considerably. Ductile behavior is essential at these crucial sites to prevent complete structural collapse under sustained loading.

Destruction from the 1994 Northridge, 1995 Kobe, and 1999 Kocaeli earthquakes[1-3] has highlighted the worldwide vulnerability of reinforced concrete columns exposed to inelastic conditions. Specifically at risk are columns in existing structures constructed prior to 1971 that have substandard seismic design details. The insufficient amount of transverse reinforcement renders these members ineffective at dissipating seismic energy and the inadequate ductility rapidly leads to failure. Typical procedures to compensate for the deficiencies involve external retrofitting of these columns with steel or concrete overlays. Experiments[4] have established that the additional confinement provided improves seismic performance, especially within the potential plastic hinging zones. An innovative retrofit technique using carbon fiber-reinforced polymer (CFRP) and glass fiber-reinforced polymer (GFRP) has emerged as an attractive alternative to conventional upgrading measures. Assembled fabric sheets consisting of synthetic fibers are impregnated with a resinous matrix and applied to the concrete section. Their light weight enables installation to be accomplished quickly with minimal labor resources and service disruptions. These materials also exhibit resistance to corrosion in chloride environments that can reduce maintenance costs. Columns strengthened with fiber-reinforced polymer (FRP) composites also experience lower associated stiffness increases compared with the traditional rehabilitation methods.

In recent years, external FRP systems have become widespread in field column applications despite only limited experimental research data on the seismic response of FRP-wrapped specimens. The objective of the current study is to determine the effectiveness of CFRP and GFRP to strengthen reinforced concrete columns, subjected to simulated earthquake loading, using both upgrade and repair strategies. This research is a component of a comprehensive investigation to decipher the effects of confinement reinforcement on the seismic behavior of circular and square concrete columns.[5,6] Selected results from a recent test series are presented in this paper to evaluate the performance of columns confined with CFRP. Comparisons are also made between the effectiveness of CFRP and of transverse steel to provide seismic resistance.

RESEARCH SIGNIFICANCE

Few studies have investigated the seismic behavior of realistic square columns wrapped with CFRP. This study provides relevant seismic performance data on near full-scale columns typical of existing infrastructure. The reported research addresses the repair of damaged columns with CFRP, a topic of extreme importance for the engineering industry. Jacket effectiveness is also evaluated directly through comparisons of strengthened-column responses with those of similar columns reinforced solely with transverse steel adhering to ACI earthquake provisions.[7] Results can be used in the development of design guidelines for retrofitting with CFRP.

EXPERIMENTAL PROGRAM

Eight large-scale columns were designed with nonseismic transverse steel detailing. The main variables studied were the number of CFRP layers in the test zone, the presence of column damage, and the level of applied axial load. Retrofitted and control specimens were tested under a constant axial load with cyclic flexural and shear loads to simulate seismic loading conditions.

ACI Structural Journal, V. 100, No. 6, November-December 2003.
MS No. 02-341 received September 9, 2002, and reviewed under Institute publication policies. Pertinent discussion including author's closure, if any, will be published in the September-October 2004 *ACI Structural Journal* if the discussion is received by May 1, 2004.

Richard D. Iacobucci *is a research assistant in structural engineering at the University of Toronto, Toronto, Ontario, Canada. He received his BASc and MASc in 1998 and 2001, respectively, from the University of Toronto.*

Shamim A. Sheikh, *FACI, is a professor of civil engineering at the University of Toronto. He is a member and former Chair of Joint ACI-ASCE Committee 441, Reinforced Concrete Columns, and a member of ACI Committee 374, Performance-Based Seismic Design of Concrete Buildings. In 1999, he received the ACI Structural Research Award for a paper on the design of ductile concrete columns. His research interests include earthquake resistance and seismic upgrade of concrete structures, confinement of concrete, use of fiber-reinforced polymers in concrete structures, and expansive cement and its applications.*

Oguzhan Bayrak *is an assistant professor of civil engineering at the University of Texas at Austin, Austin, Tex. He is Chair of Joint ACI-ASCE Committee 441, Reinforced Concrete Columns, and a member of ACI Committee 341, Earthquake-Resistant Concrete Bridges. His research interests include confinement of concrete, seismic design of reinforced concrete members, inelastic buckling of reinforcing bars in concrete columns, performance-based design of concrete columns, repair and upgrade of concrete structures with fiber-reinforced polymers, and strut-and-tie modeling.*

Table 1—Details of test specimens

Specimen	f'_c, MPa	Layers of CFRP	Lateral steel				Axial load	
			Size at spacing, mm	ρ_s, %	f_y, MPa	$A_{sh}/A_{sh(ACI)}$	$P/f'_c A_g$	P/P_o
AS-1NS	31.4	0	U.S. No. 3 at 300	0.61	457	0.49	0.40	0.33
ASC-2NS	36.5	1	U.S. No. 3 at 300	0.61	457	0.42	0.38	0.33
ASC-3NS	36.9	2	U.S. No. 3 at 300	0.61	457	0.42	0.65	0.56
ASC-4NS	36.9	1	U.S. No. 3 at 300	0.61	457	0.42	0.65	0.56
ASC-5NS	37.0	3	U.S. No. 3 at 300	0.61	457	0.42	0.65	0.56
ASC-6NS	37.0	2	U.S. No. 3 at 300	0.61	457	0.42	0.38	0.33
AS-7NS	37.0	0	U.S. No. 3 at 300	0.61	457	0.42	0.38	0.33
ASCR-7NS	37.0	1	U.S. No. 3 at 300	0.61	457	0.42	0.38	0.33
AS-8NS	42.3	0	U.S. No. 3 at 300	0.61	4.57	0.36	0.62	0.56
ASCR-8NS	42.3	3	U.S. No. 3 at 300	0.61	457	0.36	0.62	0.56
AS-3*	33.2	0	U.S. No. 3 at 108	1.68	507	1.43	0.60	0.50
AS-19*	32.3	0	U.S. No. 3/ 6 mm at 108	1.30	507/ 462	1.12	0.47	0.39

*From Sheikh and Khoury.[8]

Table 2—Properties of reinforcing steel

Bar size	Stress-strain characteristics						
	f_y, MPa	ε_y	E_s, MPa	ε_{sh}	f_u, MPa	ε_u	ε_r
U.S. No. 3	457	0.0022	207,730	0.0070	739	0.1050	0.1435
20M	465	0.0023	202,170	0.0113	640	0.1288	0.2038
10M	505	0.0028	180,360	0.0133	680	0.1413	0.2163

Specimens

Each specimen was comprised of a 305 x 305 x 1473 mm column connected to a 508 x 762 x 813 mm stub. The corners of all columns were rounded using concave wood sections, with a 16 mm radius, placed inside the forms during casting to facilitate FRP wrapping. The columns were characteristic of field members located in multistory building frames or in bridges between the points of maximum moment and contraflexure. Each stub was adjacent to the site of maximum moment and served as a discontinuity such as a column-footing junction or a beam-column interface. All specimens contained eight 20M longitudinal bars (ρ_g = 2.58%) uniformly distributed around the column core creating a core area that was 77% of the gross column area. Perimeter hoops laterally supported the four corner bars and internal hoops enclosed the four middle bars. Details of the specimens are listed in Table 1 and Fig. 1. The first letter, A, of the identification label represents the transverse steel configuration depicted in the figure. The second letter, S, indicates the presence of a stub, while the letter C means the column was wrapped with CFRP in the test zone. The combination CR reveals that an unwrapped specimen was first damaged, then repaired with CFRP and tested again to failure. The number identifies the testing sequence while the NS term refers to the use of normal strength concrete.

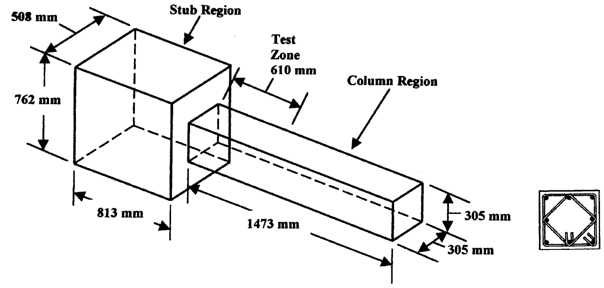

Fig. 1—Geometry and steel configuration of specimens.

Concrete and grout

Seven columns were cast together with one batch of concrete. The eighth column (AS-8NS) was added later to the program and cast separately. Each cast used a ready-mixed concrete design consisting of Type 10 portland cement, crushed limestone with a 10 mm maximum size, and a nominal 28-day target strength of 25 MPa. An initial concrete slump of approximately 140 mm was achieved through the addition of high-range water-reducing admixture prior to casting. The specimens were cast vertically and rod vibrators increased concrete compaction. Testing of 36 standard cylinders from each pour helped monitor the strength development of concrete with age. The concrete strength f'_c for each specimen listed in Table 1 was obtained from the strength-age relationship.

A nonshrink structural grout with aggregate was used during the repair phase of the study for two specimens. Its water-cement ratio (w/c) was maintained at 0.22 to assure adequate workability for placement. Compressive strength reached 37 and 42 MPa at 7 and 12 days, respectively, corresponding to the original concrete strengths of the two repaired specimens.

Steel

The specimens were formed using three different types of reinforcing steel. Longitudinal reinforcement consisted of eight 20M bars, rectilinear and diamond column ties were created from U.S. No. 3 bars, and stub stirrups were composed of 10M bars. Table 2 lists the critical stress-strain characteristics of all steel reinforcement. f_y and f_u are the stress levels at yielding and the ultimate condition, respectively; ε_y, ε_{sh}, ε_u, and ε_r identify the strain levels at yielding, the start of strain hardening, the ultimate condition, and rupture, respectively.

Reinforcing cages

The structural skeleton of each specimen was comprised of two components: a column cage and a stub cage (Fig. 2). These were assembled separately and then attached to each other creating an interconnected specimen. The longitudinal steel extended through the stubs to 15 mm from the end. The U.S. No. 3 lateral ties were spaced at 300 mm to represent

Table 3—Properties of FRP composites

Composite	Thickness, mm	Tensile strength/ unit width (N/mm/layer)	Strain at rupture	Elastic modulus,* MPa
CFRP	1.00	962	0.0126	76,350
GFRP	1.25	563	0.0211	21,346

*Values shown based on theoretical thicknesses.

typical pre-1971 column design details within the 610 mm-long test zone adjacent to the stub. Spacing outside this region was reduced to 150 mm to decrease the failure potential beyond the critical zone. Stub reinforcement consisted of 10M horizontal and vertical stirrups at 64 mm spacing. Additional 10M bars with 135-degree hooks were added at two sides to increase stub stiffness.

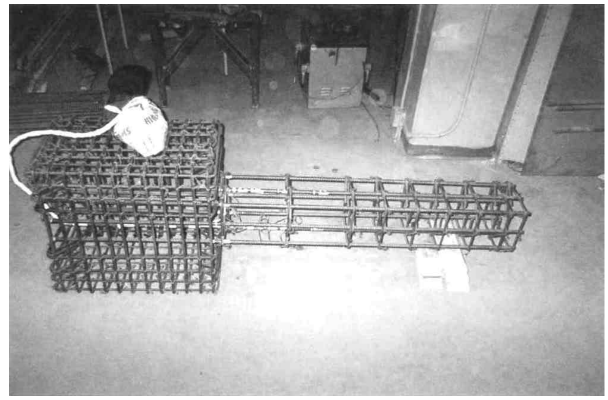

Fig. 2—Typical reinforcing cage.

FRPs

All designated specimens were retrofitted using a commercially available fiber wrap system. Two types of FRP composites were used to strengthen deficient and repair damaged columns as shown in Fig. 3. The main composite used within the test zone consisted of 1.0 mm CFRP fabric (610 mm wide) while 1.25 mm GFRP fabric (914 mm wide) covered the remaining column area. GFRP was used to economically reduce the likelihood of failure outside of the test region and was not a focus of the test series. The mechanical properties of the composites, given in Table 3, were ascertained from tensile tests of composite coupons.

Both sheet types were applied observing strict quality control procedures. The epoxy was mixed using two components (A and B) at a volumetric ratio of 100 parts A to 42 parts B. Lengths of fabric were placed on plastic sheets and saturated with epoxy using a rolling brush. The column surface was then thoroughly coated with epoxy to improve the concrete-fabric bond and the impregnated fabric was hand wrapped around the column with fiber orientation in the lateral direction. Care was exercised to ensure each composite layer was tightly wrapped without entrapped air pockets or fabric distortions.

It should be noted that threaded rods, crucial for installing testing instrumentation, had been placed within the test zone prior to casting concrete. To maintain clear openings to these rods, holes in the CFRP were made by separating the wrap fibers at all rod locations as each layer was forced against the column. An additional CFRP strip (76 x 585 mm) was used to strengthen each of the four lines of embedded rods. Regardless of the number of CFRP or GFRP layers applied (Table 1), a 152 mm overlap was added at the end for bond integrity. A strip of GFRP (152 x 1346 mm) was also placed at the CFRP-GFRP interface. Each retrofitted specimen was permitted to cure for at least 6 days to ensure full strength gain before testing.

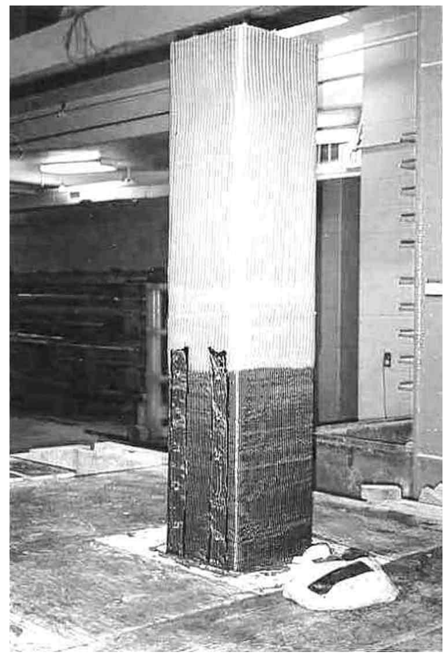

Fig. 3—Typically retrofitted column.

Instrumentation

All specimens were instrumented during testing to monitor strains at several locations, deflections along the specimen length, and load levels. Local strains on both longitudinal and lateral steel were measured using a total of 36 electric strain gages. Six longitudinal bars had one gage while the two remaining bars each had seven gages. Two lateral tie sets adjacent to the stub contained 16 gages. CFRP jacket strains were obtained with eight surface strain gages oriented in the direction of carbon fibers; each column face had two gages positioned on the longitudinal centerline at 130 and 240 mm, respectively, from the stub face. Longitudinal deformations of the concrete core within the test zone were obtained from 18 linear variable differential transducers (LVDTs) attached to the embedded threaded rods. Distances between these LVDTs varied from 75 to 220 mm, allowing external monitoring of strains along a distance of 515 mm. Lateral displacements at six different span locations were also monitored using LVDTs.

Testing

Each specimen was tested horizontally in the loading frame shown in Figure 4 under a constant axial load and applied lateral cyclic displacement excursions simulating earthquake forces. A hydraulic jack with a capacity of 4450 kN provided the axial force that was measured using a load cell of similar capacity. Special hinges permitted in-plane rotation of each specimen end allowing the loading path to remain constant throughout the test. Engineering levels were used to initially align each specimen in both the vertical and horizontal planes. The specimen was axially loaded in 200 kN increments up to 50% of the specified test load (Table 1) and readings from instrumentation were checked at each stage. If an adjustment was required to obtain the necessary alignment, the specimen was unloaded and repositioned. The process was repeated until the column was properly aligned in the

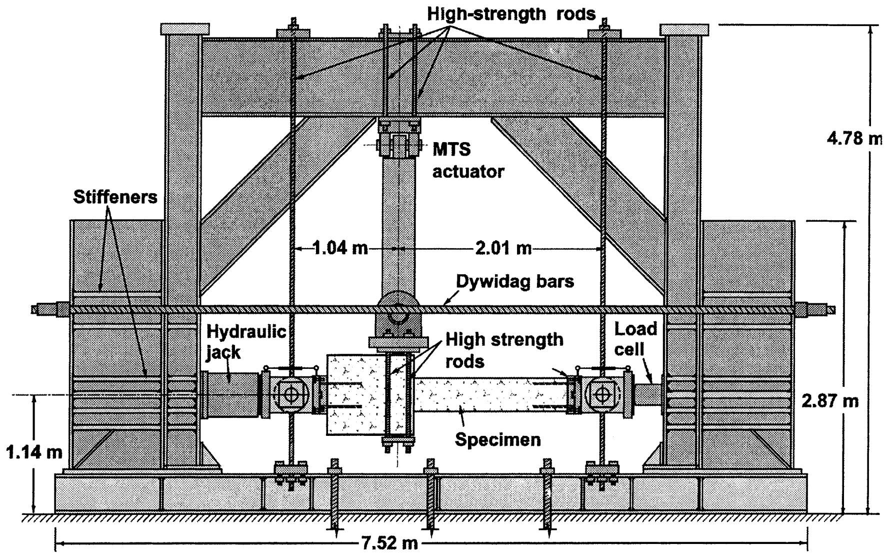

Fig. 4—Test frame for cyclic loading.

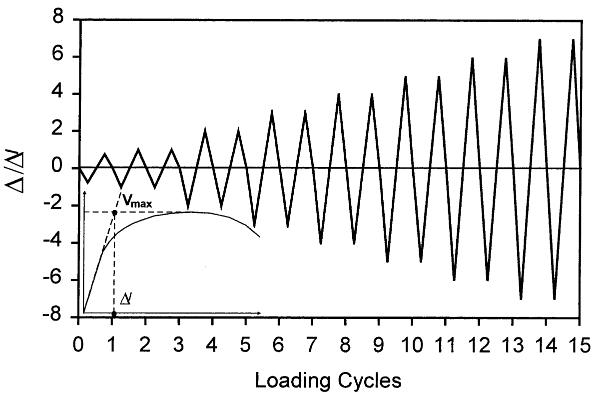

Fig. 5—Specified lateral displacement loading.

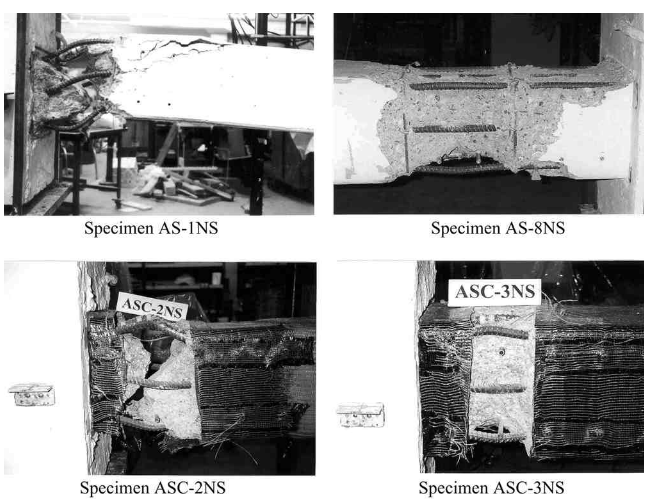

Fig. 6—Specimens at end of testing.

test frame, although most specimens required minimal adjustment. After alignment, the predetermined axial load was applied and the 1000 kN actuator was connected to the stub adjacent to the interface with the column.

The specimen was then subjected to transverse displacement excursions (Fig. 5) using a displacement-control mode of loading. The first cycle exposed the specimen to 75% of the elastic or yield displacement Δ'; the displacement Δ' is also defined in Fig. 5. It represents the lateral deflection corresponding to the maximum lateral load V_{max} on a straight line joining the origin and a point at 65% of V_{max}.[9] It should be noted that Δ' was determined using the theoretical sectional behavior of the column and integrating curvatures along its length. The subsequent cyclic displacement excursions were gradually increased and the test was terminated when the specimen was unable to support the originally applied axial load.

While the strengthened specimens were wrapped with CFRP before the application of any load, the procedure was slightly modified for specimens chosen to undergo repairs. Each member was cycled until, at minimum, yielding of longitudinal steel initiated and concrete cover spalling occurred. Once damage was deemed acceptable, the column was returned to a zero lateral displacement position and remained within the test frame under a reduced axial load. The damaged columns were repaired with structural grout and permitted to cure for at least 48 h before being jacketed with FRP. Column AS-7NS/ASCR-7NS was repaired while subjected to an axial load equal to 76% of the original value. Column AS-8NS/ASCR-8NS was inadvertently damaged more than what was anticipated. Therefore, no axial load was applied on this column during the repair process. Following a retrofit curing period of at least 6 days, the specimen was subjected to excursions commencing at $0.75\Delta'$ (Fig. 5) under the original axial loading until failure occurred.

RESULTS

Test observations

Damage sustained within the test zones of unwrapped specimens (Fig. 6) first appeared as hairline cracks in the top and bottom concrete covers. Additional cracks emerged and existing cracks widened as the size of lateral displacement excursions increased. Vertical flexural cracks formed during the first three cycles at a distance of 300 to 400 mm from the face of the stub and occurred in later stages closer to the column-stub interface. These cracks rapidly developed into flexural-shear cracks as they propagated through the column sides. Concrete cover spalled at the peak of the 6th loading cycle in Specimens AS-1NS and AS-7NS, and during the 4th loading cycle for Specimen AS-8NS. Cover spalling for the columns extended over a distance that varied from 245 to 715 mm. While Specimen AS-7NS was lightly damaged, control Specimens AS-1NS and AS-8NS were severely damaged experiencing

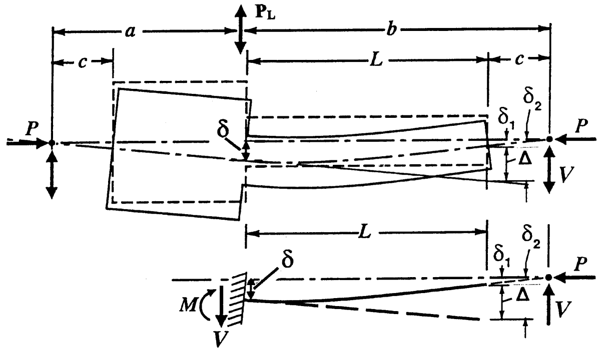

Fig. 7—Idealization of test specimens.

yielding of lateral ties followed by initiation of longitudinal bar buckling. The behavior of all columns was dominated by flexural-shear effects while primary damage zones for Specimens AS-1NS, AS-7NS, and AS-8NS concentrated at 185, 190, and 460 mm, respectively, from the stub's face.

Retrofitted specimens produced sporadic popping sounds during the tests as the hardened composite jackets were stressed. Increments in lateral excursions magnified both the sounds and the visible deflection occurring at the hinging zone. Several composite ridges perpendicular to the plane of bending first appeared at approximately 15 and 350 mm from the column-stub interface, and more ridges appeared between these regions as displacements increased. Delamination of the CFRP jacket from the concrete spread into the column sides while cracks formed in the composite mainly along the ridges. Yielding of transverse reinforcement tended to occur at lateral displacements of $3\Delta'$ to $5\Delta'$ for columns with high axial load and at $6\Delta'$ to $8\Delta'$ for lightly loaded specimens. Substantial dilation of the CFRP-wrapped region was observed over the last few cycles of each test. The longitudinal reinforcement buckled during the final loading sequence and rupture of CFRP fibers was initiated at or near one of the column corners. A thunderous noise accompanied the release of previously generated pressure, particularly during high axial load tests, and column failure ensued. Figure 6 shows typical damage for retrofitted columns. The most extensive damage generally coincided with the location of first fiber rupture that occurred in different specimens at 125 to 195 mm from the column-stub junction; the corresponding location for Specimen ASCR-8NS was 415 mm. Although most columns experienced flexural failures, shear effects appeared to dominate the final cycles of Specimens ASC-2NS and ASC-4NS. It was also observed that the two bottom corner longitudinal bars of Specimen ASC-6NS fractured adjacent to the stub during the 17th loading cycle.

Specimen behavior

Figure 7 depicts the idealization of the test specimens showing all forces to which each was subjected. Responses are presented in Fig. 8 to 17 with key events during the tests clearly marked. Figures are in the form of moment M versus curvature ϕ plots representing section behavior; shear force V versus tip deflection Δ relationships illustrating member behavior were also developed. The M-versus-ϕ response is more crucial because deformations concentrate at the critical sections within the plastic hinge regions during post-elastic loading.

Values of V were calculated from the measured applied lateral load P_L and Δ readings were obtained from the column-stub interface displacement δ. Although the interface was subjected

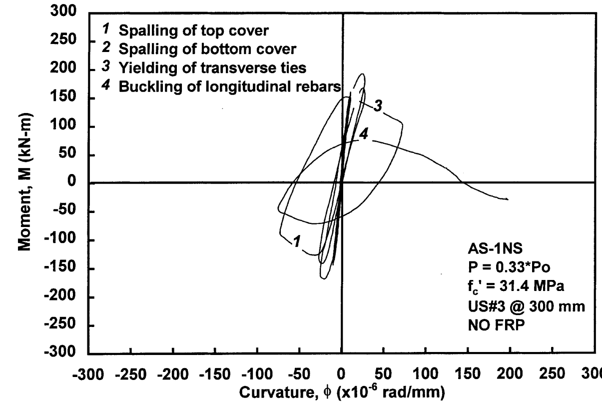

Fig. 8—Moment-versus-curvature behavior of Specimen AS-1NS.

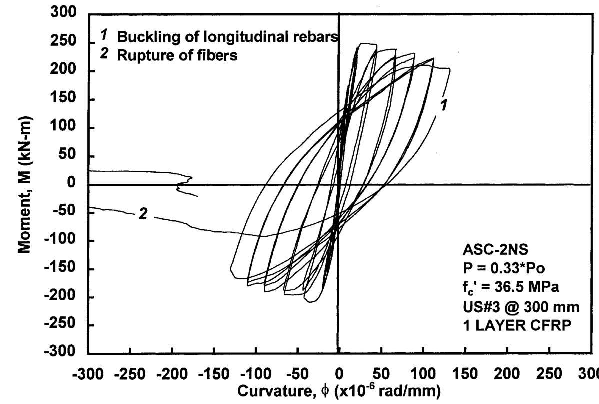

Fig. 9—Moment-versus-curvature behavior of Specimen ASC-2NS.

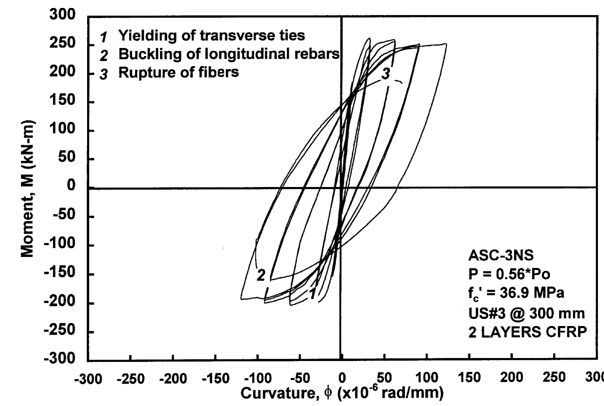

Fig. 10—Moment-versus-curvature behavior of Specimen ASC-3NS.

to the maximum moment, column failure shifted away from this zone due to the confinement provided by the stub. Therefore, all M values are those at failed sections and include the axial load contribution using the failed section deflection Δ_f calculated from the deflected column shape. The ϕ values were obtained from deformation readings of top and bottom LVDTs located at the critical sections. Table 4 lists peak forces and the most damaged section for all specimens.

Ductility parameters

Several empirical member and section parameters from the research of Khoury and Sheikh[9] (Fig. 18) were used in this study to investigate the performance of all test specimens. The displacement and curvature ductility factors μ_Δ and

Table 4—Experimental values and calculated capacities

Specimen	Layers of CFRP	P/P_o	V_{max}, kN	V_r, kN	M_{smax}, kN · m	M_{max}, kN · m	M_{pr}, kN · m	Damage zone, mm
AS-1NS	0	0.33	108.2	111.0	200.3	180.4	200.3	185
ASC-2NS	1	0.33	127.5	113.2	252.4	228.8	214.6	175
ASC-3NS	2	0.56	126.4	113.3	255.9	233.2	177.1	180
ASC-4NS	1	0.56	120.7	113.3	236.9	218.2	177.1	185
ASC-5NS	3	0.56	131.3	113.4	281.3	260.1	177.6	195
ASC-6NS	2	0.33	129.6	113.4	262.3	245.8	216.2	125
AS-7NS	0	0.33	117.2	113.4	230.0	208.4	216.2	190
ASCR-7NS	1	0.33	118.1	113.4	237.4	215.8	216.2	180
AS-8NS	0	0.56	105.7	115.4	210.3	167.6	189.7	460
ASCR-8NS	3	0.56	113.4	115.4	242.2	198.0	189.7	415
AS-3*	0	0.50	97.0	286.9	204.0	192.9	170.0	140
AS-19*	0	0.39	108.5	213.1	219.6	202.1	185.7	114

*From Sheikh and Khoury.[8]

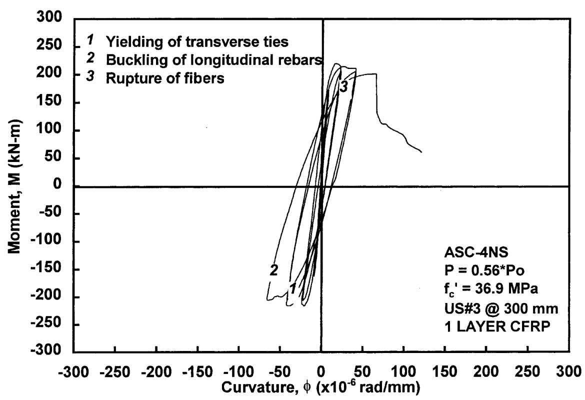

Fig. 11—Moment-versus-curvature behavior of Specimen ASC-4NS.

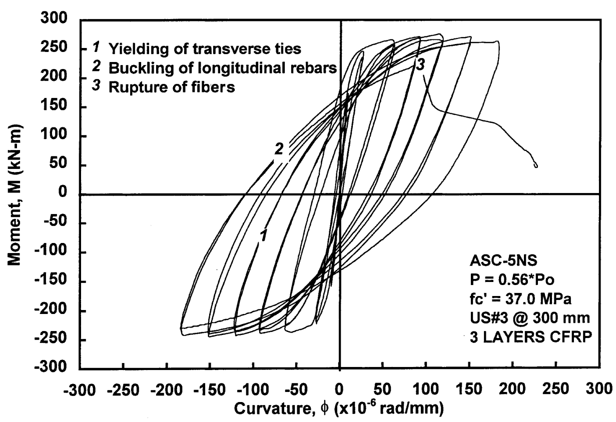

Fig. 12—Moment-versus-curvature behavior of Specimen ASC-5NS.

μ_ϕ, along with the cumulative ductility ratios N_Δ and N_ϕ, represent the deformability of a concrete member and section, respectively. Both work-damage indicator W and energy-damage indicator E quantify the energy dissipation capacities of an entire member and specific hinging section, respectively; these provide an estimate of toughness. Table 5 presents parameter values for a 10% (subscript 90) and 20% (subscript 80) reduction in moment or shear forces beyond the peak and until the end of the test (subscript t).

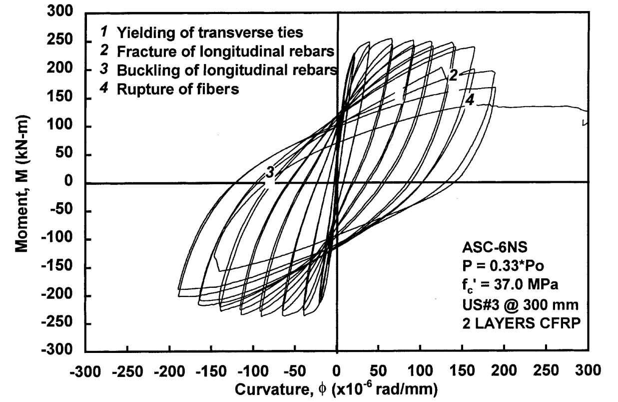

Fig. 13—Moment-versus-curvature behavior of Specimen ASC-6NS.

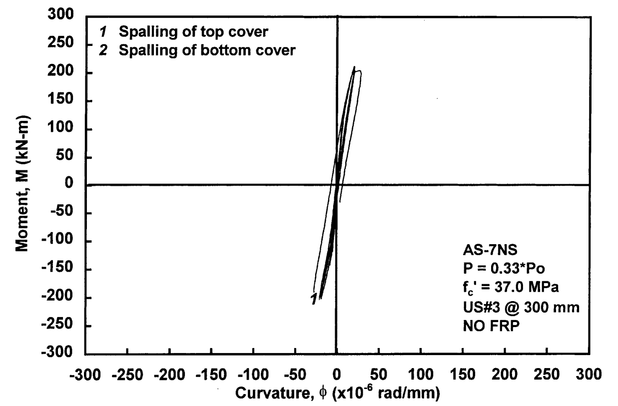

Fig. 14—Moment-versus-curvature behavior of Specimen AS-7NS.

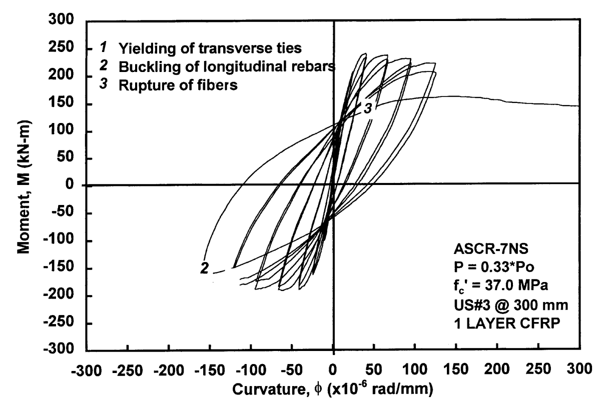

Fig. 15—Moment-versus-curvature behavior of Specimen ASCR-7NS.

DISCUSSION OF RESULTS

A general overview of the responses indicates that a range of inelastic performance levels exists. Some specimens dissipate large amounts of energy over several cycles and are very ductile while others deteriorate soon after testing commences. Individual behaviors seem to depend on the number of CFRP layers, the presence of damage prior to retrofitting, and the level of constantly applied axial load.

Effect of CFRP retrofitting on deficient columns

The influence of strengthening deficiently built square columns with CFRP is evaluated using comparisons of similar

Table 5—Member and section ductility values

Specimen	Ductility factors			Ductility ratios				Energy indicators			
	$\mu_{\Delta 80}$	$\mu_{\phi 80}$	$\mu_{\phi 90}$	$N_{\Delta 80}$	$N_{\Delta t}$	$N_{\phi 80}$	$N_{\phi t}$	W_{80}	W_t	E_{80}	E_t
AS-1NS	3.7	5.3	4.1	9.5	18.4	8.4	23.9	10.2	25.3	10.8	66.2
ASC-2NS	6.1	11.6	9.1	33.3	61.1	61.2	72.8	110.5	254.6	352.1	465.8
ASC-3NS	5.6	+	+	23.6	34.5	+	56.0	80.9	130.9	+	326.2
ASC-4NS	5.2	+	+	15.9	21.6	+	24.3	41.4	57.1	+	79.2
ASC-5NS	7.1	+	+	44.5	59.2	+	109.3	260.6	392.1	+	1083.2
ASC-6NS	8.2	+	15.4	59.2	104.4	+	160.5	306.7	621.9	+	1328.1
AS-7NS	+*	+	+	+	12.0	+	9.9	+	13.5	+	7.7
ASCR-7NS	5.4	+	+	35.3	41.4	+	55.9	127.3	139.9	+	214.7
AS-8NS	+	+	+	+	7.3	+	5.4	+	5.4	+	7.9
ASCR-8NS	+	+	+	+	30.7	+	27.9	+	145.4	+	101.7
AS-3†	4.7	+	+	23.0	32.0	+	74.0	84.0	127.0	+	753.0
AS-19†	4.0	19.0	10.0	18.0	44.0	85.0	129.0	33.0	130.0	631.0	1230.0

*+ = moment or shear did not drop to this level.
†From Sheikh and Khoury.[8]

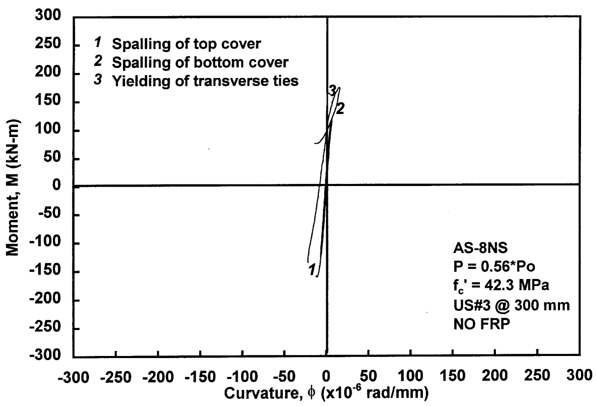

Fig. 16—Moment-versus-curvature behavior of Specimen AS-8NS.

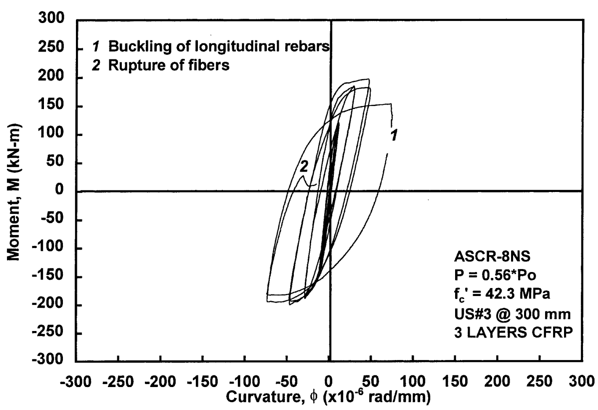

Fig. 17—Moment-versus-curvature behavior of Specimen ASCR-8NS.

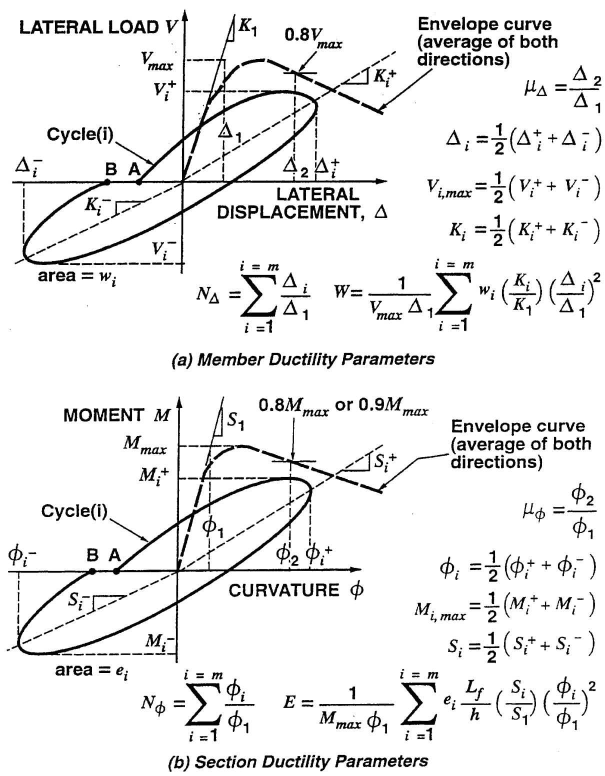

Fig. 18—Ductility parameters from Khoury and Sheikh.[9]

specimens tested under identical loading conditions. Specimens AS-1NS, ASC-2NS, and ASC-6NS contained similar insufficient quantities of seismic transverse steel compared with code requirements (ACI 318-02[7]). Each column was subjected to an axial load that was 33% of the nominal column capacity P_o. This load level represented a force slightly higher than the balanced load in each case. While Specimen AS-1NS served as the control column, Specimens ASC-2NS and ASC-6NS were retrofitted with one and two CFRP layers, respectively. Table 5 clearly shows that all comparable ductility parameters for the retrofitted columns are greater than those for the unwrapped specimen. Specimens ASC-2NS and ASC-6NS also demonstrated energy dissipation capacities that were an average of 15 and 25 times greater, respectively, than those for Specimen AS-1NS. The enhanced cyclic performance of the wrapped columns is obvious from the M-versus-ϕ relationships (Fig. 8, 9, and 13) that show decreased rates of stiffness and strength deterioration when CFRP is present. Specimens ASC-2NS and ASC-6NS were able to sustain 15 and 20 cycles, respectively, while Specimen AS-1NS failed following the 7th cycle. The performance of Specimen ASC-6NS was so improved that the column continued sustaining load for three additional cycles following fracture of two longitudinal bars. The CFRP jackets provided extra confinement to the column hinging zones and reduced the adverse impact of inadequate lateral steel content.

A second set of comparable columns that provide insight concerning CFRP retrofitting are Specimens AS-8NS, ASC-4NS, ASC-3NS, and ASC-5NS wrapped with 0, 1, 2, and 3 CFRP layers, respectively. These columns possessed a similar insufficient fraction of ACI-required seismic reinforcement[7] to confine the concrete core (36 to 42%). Axial load level remained at 56% of P_o during testing and represents the upper limit dictated in most building codes. A general survey of the values for ductility parameters in Table 5 reveals a substantially improved inelastic response for all upgraded columns. Particularly impressive are the energy dissipation quantities that are an average of 10 to 105 times larger than the corresponding control values. Specimens ASC-4NS, ASC-3NS, and ASC-5NS remained structurally sound for 8, 11, and 15 lateral excursions, respectively. In contrast, Specimen AS-8NS could only endure four loading cycles before being severely damaged. Figure 10, 11, 12, and 16 illustrate that seismic performance progressively improved as the number of CFRP layers increased. Restraint provided to the concrete core was augmented with each layer added, permitting upgraded specimens to undergo greater inelastic deformations before CFRP rupture commenced.

The jackets also had a pronounced impact on maximum shear and moment forces (V_{max} and M_{max}) for all strengthened specimens. Table 4 shows experimental levels recorded from each test along with shear capacity V_r and probable moment capacity M_{pr} levels as calculated from seismic provisions of the CSA A23.3-94 code.[10] It should be noted that these calculations account for steel and concrete contributions only; one layer of CFRP adds over 500 kN of shear capacity to the column section. Examination of shear values indicates that strengthened specimens attained V_{max} quantities 14 to 24% higher than the corresponding control column quantities. Furthermore, wrapped specimens were subjected to shear forces that were 7 to 16% higher than V_r forces while V_{max} for each control column was smaller than the V_r specified. It is evident that CFRP layers mitigated the effects of large transverse steel spacing within the hinging zone and enhanced shear strength in addition to improving the ductility performance and flexural strength. Retrofitted columns showed increases in M_{max} levels of 27 to 55% over control column levels and from 7 to 47% over M_{pr} values. While higher concrete strengths for Specimens ASC-2NS and ASC-6NS are likely responsible for some of the moment augmentation over their control column (AS-1NS), the large magnitude of the improvements was due to CFRP strengthening. It is also obvious that M_{max} quantities for control columns did not reach expected M_{pr} quantities. Once CFRP jackets were implemented, confinement was significantly increased and columns were therefore permitted to surpass calculated moment forces.

An overview of the two column sets discussed above reveals that CFRP wraps can transform square column behavior from that associated with brittle action to that consistent with flexural responses. The higher ductility levels and energy dissipation capacities observed suggest that CFRP-strengthening of deficient columns in current infrastructure could improve their seismic performance. The visible presence of shear effects during the final excursions for Specimens ASC-2NS and ASC-4NS, however, arouses suspicion that one CFRP layer might be insufficient to ensure flexure-dominated failures occur. The added amount of moment capacity among all wrapped columns may also be undesirable because higher seismic forces could be transmitted to adjacent structural elements and cause failure away from the retrofitted zone. Regardless of the number of layers, the retrofit procedure may have to include reinforcement of the beam-column joints that are likely critical locations of failure during a seismic event.

Effect of CFRP retrofitting on damaged columns

Performance features of the CFRP repair scheme are identified through a comparison of Specimen ASC-2NS with Specimen ASCR-7NS. Both had 42% of the lateral steel content mandated in ACI seismic provisions[7] and each carried an identical axial load of $0.33P_o$. Specimen ASC-2NS was tested with one CFRP layer added while Specimen ASCR-7NS was first lightly damaged as an unretrofitted column (AS-7NS) before being retrofitted with one CFRP layer and retested to failure. The parameters recorded in Table 5 indicate Specimen ASCR-7NS displayed ductility that was comparable with Specimen ASC-2NS up to an approximately 20% drop in capacity beyond the peak. The total ductility parameters, however, were significantly lower for Specimen ASCR-7NS. Hysteresis loops presented (Fig. 9 and 15) confirm the behavior of the repaired column was subordinate to, yet closely resembled, that of the undamaged wrapped specimen both in number of excursions and ultimate strength quantities. The substantial difference in the total ductility parameters reflects previous damage sustained during cycling of Specimen AS-7NS prior to retrofit. Nevertheless, the CFRP repair restored much of the inherent seismic capabilities of Specimen ASCR-7NS and vastly improved its performance compared with its unretrofitted control column AS-1NS (Fig. 8).

While the previous discussion identifies merits of CFRP rehabilitation in a lightly damaged case, focusing on the response of Specimens ASC-5NS and ASCR-8NS clarifies repair limitations at a higher damage state. Specimen ASC-5NS was wrapped with three plies of CFRP and subjected to an axial load of $0.56P_o$. Specimen ASCR-8NS incurred extensive structural damage without retrofit (AS-8NS) under the same high axial load prior to acquisition of a three-layer jacket and exposure to further lateral excursions. Although each column had similar concrete strengths and seismic hoop requirements, Specimen ASCR-8NS displayed a thoroughly inferior performance (Fig. 12 and 17). Available ductility, toughness, and maximum strength values for the repaired column were subordinate to values for Specimen ASC-5NS, despite exceeding those for Specimen AS-8NS. The data suggests that three CFRP layers were insufficient to fully compensate for the previous damage and Specimen ASCR-8NS failed prematurely.

Retrofitting square columns with CFRP jackets appears to positively influence seismic behavior of previously degraded members although the amount of damage sustained greatly affects their repair potential and salvageability. The data also imply that more CFRP layers are required for a heavily damaged column to approach performance levels similar to those gained in an undamaged retrofitted case. But the fact that repaired specimens were seismically superior to their control unwrapped column counterparts shows that repair with CFRP jacketing in field applications holds promise. The technique would be particularly useful for restoring columns within structures that have been lightly damaged from an earthquake. Engineers could have buildings with limited damage rehabilitated quickly to at least pre-earthquake capabilities and declared safe for expeditious reoccupation, avoiding extensive structural modifications.

Stub effect

As previously stated, the maximum moment occurred at the column-stub interface. Failure, however, initiated at a location away from the stub where moment values were an average 11% less in magnitude (Table 4). It is believed that the stub provided additional confinement to the adjacent column section and reduced its tendency of lateral expansion. The moment capacity of this section therefore increased and the critical section shifted to the zone where external restraint from the stub was minimal. A direct implication is that for earthquake resistance using the capacity design method, adjustments might be required to determine the design shear force adjacent to a zone of significant confinement in a CFRP-wrapped column. Design shear could be calculated using the moment capacity available at the plastic hinges with an appropriately reduced column length if the increased capacity at interfaces is unknown. These findings concur with those obtained in similar investigations[6,8,9,11] of steel confined concrete columns with stubs.

Axial load effect

A comparison of strengthened columns that were similar to each other in all respects except for axial load level demonstrates the role of applied force on CFRP requirement. Specimen ASC-3NS was tested under a high axial load ($0.56P_o$) while Specimen ASC-6NS supported less of its maximum nominal capacity ($0.33P_o$). Although indistinguishable in assembly and retrofitting, ductility ratios shown by Specimen ASC-3NS were an average of 64% lower than those for Specimen ASC-6NS (Table 5). Furthermore, juxtaposing Fig. 10 and 13 highlights the reduced performance of Specimen ASC-3NS that resulted in 76% less energy dissipation, on average, compared with the amount transmitted into the plastic hinge of Specimen ASC-6NS. Higher demand was placed on the two CFRP layers restraining Specimen ASC-3NS under larger axial load. Specimens ASC-4NS and ASC-2NS were also similar to one another, with the main exception being axial loads of $0.56P_o$ and $0.33P_o$, respectively. The column resisting high load again experienced declines in ductility ratios (61%) and dissipated energy (74%). Its excursion limit was also reduced to eight cycles from 15 for Specimen ASC-2NS (Fig. 9 and 11) as the confinement ability of the single CFRP layer was taxed. In all cases, increases in axial loads contributed to the detriment of seismic response and increased the demand on CFRP jacketing. The destructive nature of high loading conditions in conventionally reinforced columns is well-documented[6,8,9,11] and the current results appear to support this assessment. Predictably, the study also illustrated that more CFRP layers were required for columns resisting a high axial load than for those subjected to a lower axial load to obtain similar responses. Regardless of the ductility or toughness parameters considered, there was a positive relationship between improved column performance and increasing CFRP retrofit layers. Procedures used to determine the necessary amount of CFRP retrofitting should therefore incorporate the axial force into calculations due to its overall significance.

Columns with CFRP jackets versus columns with steel transverse reinforcement

The behavioral improvements of CFRP-wrapped columns are considered particularly significant when they are examined together with results obtained from similar column tests conducted by Sheikh and Khoury.[8] Some of the specimens

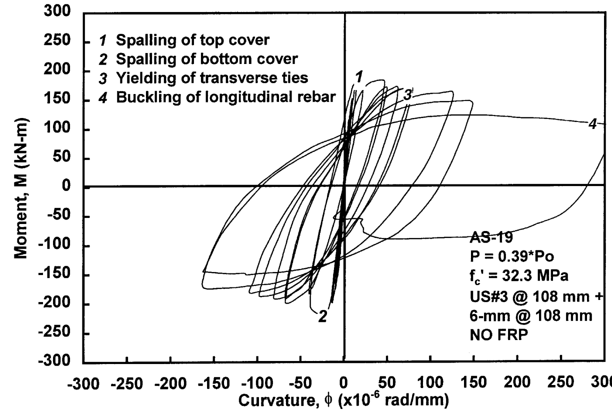

Fig. 19—Moment-versus-curvature behavior of Specimen AS-19.[8]

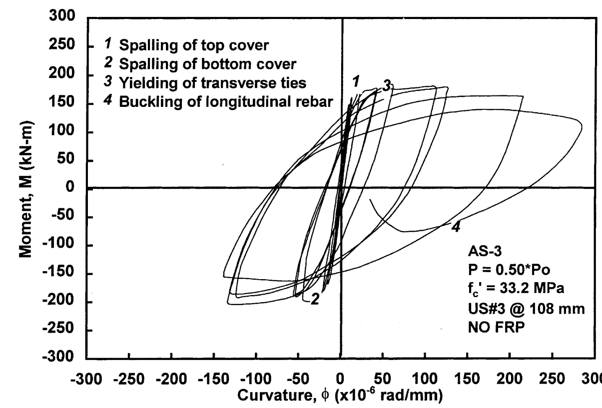

Fig. 20—Moment-versus-curvature behavior of Specimen AS-3.[8]

in that research program were laterally reinforced exclusively with steel hoops and complied with the stringent seismic requirements of the ACI building code.[7] They possessed similar material properties and had identical dimensions compared with columns of the current study. Among specimens tested at similar low axial loads, Specimen ASC-2NS retrofitted with one layer of CFRP displayed better member parameters than those of Specimen AS-19 (Table 5) and cyclic behavior was more balanced (Fig. 9 and 19); sectional parameters for the wrapped column were still lower than those for Specimen AS-19. Comparable Specimen ASC-6NS retrofitted with two layers of CFRP (Fig. 13) degraded much more gradually and resisted loading for seven cycles longer than Specimen AS-19. Most parameter values were at least 54% better as the lack of sufficient transverse steel in the retrofitted column became inconsequential (Table 5). A comparison of columns that supported similar high load levels again illustrates the success of the CFRP upgrades. Figure 10 and 20 show that Specimen ASC-3NS with two CFRP layers lasted for an equivalent number of cycles as Specimen AS-3 but achieved a generally subordinate performance with only limited gains. Conversely, Specimen ASC-5NS with three CFRP layers (Fig. 12) surpassed the behavior of Specimen AS-3. Resistance for each lateral excursion was improved as most ductility and toughness parameters exceeded by at least 44% those obtained for the code-approved column (Table 5). It is evident from these cases that appropriate retrofitting of deficient columns with CFRP can produce high-quality responses that are superior to those of columns possessing adequate steel reinforcement for seismic resistance. The level of gains observed in the strengthened specimens are encouraging given the number of deficient columns in seismic zones that could benefit from this rehabilitation procedure.

SUMMARY AND CONCLUSIONS

Reinforced concrete columns built before 1971 are known to have inadequate transverse reinforcement and can fail without sufficient warning during a major earthquake. Among the available retrofit techniques, CFRP jacketing is gaining popularity due to its ease of installation. The reported research was conducted to examine the performance of deficient and damaged columns retrofitted with CFRP under earthquake loading conditions. All the columns considered in this study are 305 mm^2. It is expected that the results obtained should be applicable to columns with different section sizes as long as parameters such as volumetric ratio of lateral steel, area of FRP confining reinforcement, and the level of axial load are appropriately scaled. The following conclusions can be drawn from this study:

1. The retrofit of seismically deficient square reinforced concrete columns with CFRP can substantially increase their ductility and energy dissipation capacities, improving seismic resistance in the process. Adverse effects from insufficient seismic steel are eliminated as CFRP jackets provide additional confinement to critical sections. Cyclic behavior progressively improves through decreases in stiffness and strength degradation rates as the number of CFRP layers increase. Shear and moment capacities can also increase as the jackets convert column performance from that consistent with brittle action to a more ductile response;

2. CFRP repair options can effectively impart ductility and enhanced seismic behavior to previously damaged columns, although the level of improvement depends on the severity of damage sustained. Thus, more CFRP layers are needed for highly degraded columns to achieve a performance similar to that of undamaged retrofitted columns;

3. Discontinuities such as footings and beam-column joints adjacent to a column appear to strengthen the column section and shift failure away from the interface to a section subjected to lower forces;

4. Higher axial forces degrade overall column response and put additional demands on CFRP jackets to restrain critical regions. A larger amount of CFRP is therefore required for columns subjected to higher axial load levels to realize similar performance enhancements as those demonstrated by retrofitted columns under lower axial loads; and

5. The seismic behavior of deficient columns appropriately retrofitted with CFRP can be superior to the response of analogous columns having sufficient lateral steel content according to earthquake building standards.

ACKNOWLEDGMENTS

The research reported herein was supported by grants from the Natural Sciences and Engineering Research Council of Canada (NSERC) and ISIS Canada, an NSERC Network of Centres of Excellence. Additional financial assistance from Fyfe and Co., R.J. Watson Inc., Premier Corrosion, and Kinectrics Inc. is greatly appreciated.

NOTATION

A_g = gross area of column, mm^2
A_{sh} = total cross-sectional area of lateral steel within spacing s, mm^2
E = energy-damage indicator
E_s = modulus of elasticity of steel, MPa
f_c' = compressive strength of concrete determined from 150 x 300 mm cylinders, MPa
f_u = ultimate strength of steel, MPa
f_y = yield strength of longitudinal steel, MPa
h = cross-sectional depth of columns, mm
L_f = length of most damaged column region, mm
M = moment sustained at most damaged column region, kN · m
M_{max} = maximum moment sustained at most damaged column region, kN · m
M_{pr} = probable moment capacity of members determined using a longitudinal tensile strength of $1.25f_y$ and neglecting all strength reduction factors, kN · m
M_{smax} = maximum moment sustained at column-stub interface, kN · m
N_Δ = cumulative displacement ductility ratio
N_ϕ = cumulative curvature ductility ratio
P = axial load applied to column sections, kN
P_L = lateral load applied to columns, kN
P_o = unconfined theoretical axial load-carrying capacity of column, kN
V = shear sustained by column, kN
V_{max} = maximum shear sustained by column, kN
V_r = theoretical shear capacity of column, kN
W = work-damage indicator
Δ', Δ_1 = lateral deflection obtained from V-Δ curve corresponding to maximum lateral load on straight line joining origin and point at 65% of V_{max}, mm
Δ_2 = lateral deflection obtained from V-Δ curve corresponding to 80% of V_{max} on descending portion of curve, mm
Δ_f = deflection at failed section, mm
δ = displacement at column-stub interface, mm
ε_r = rupture strain of steel
ε_{sh} = strain at onset of strain hardening
ε_u = strain at ultimate stress in steel
ε_y = yield strain in steel
μ_Δ = displacement ductility factor
μ_ϕ = curvature ductility factor
ρ_g = ratio of area of longitudinal steel to that of cross section, %
ρ_s = volumetric ratio of rectilinear ties to concrete core measured center-to-center of perimeter ties, %
ϕ = curvature of most damaged column region, rad/mm
ϕ_1 = curvature obtained from M-ϕ curve corresponding to maximum moment on straight line joining origin and point at 65% of M_{max}, rad/mm
ϕ_2 = curvature obtained from M-ϕ curve corresponding to 80% of M_{max} on descending portion of curve, rad/mm

REFERENCES

1. "Northridge Earthquake of January 17, 1994, Preliminary Reconnaissance Report," *EERI Publication* No. 94-01, Hall, J. F., ed., Earthquake Engineering Research Institute, Oakland, Calif., Mar. 1994, 104 pp.

2. Comartin, C. D.; Greene, M.; and Tubbesing, S. K., "The Hyogo-Ken Nanbu Earthquake: Great Hanshin Earthquake Disaster, January 17, 1995, Preliminary Reconnaissance Report," *EERI Publication* No. 95-04, Earthquake Engineering Research Institute, Oakland, Calif., Feb. 1995, 116 pp.

3. Saatcioglu, M.; Gardner, N. J.; and Ghobarah, A., "1999 Turkey Earthquake: Performance of RC Structures," *Concrete International*, V. 23, No. 3, Mar. 2001, pp. 47-56.

4. Priestley, M. J. N.; Seible, F.; and Calvi, M., *Seismic Design and Retrofit of Bridges*, John Wiley and Sons Inc., New York, 1996, 686 pp.

5. Iacobucci, R. D., and Sheikh, S. A., "Seismic Upgrade and Repair of Square Reinforced Concrete Columns with Carbon FRP Jackets," *Research Report* IS0101, Department of Civil Engineering, University of Toronto, Ontario, Canada, Sept. 2001, 165 pp.

6. Sheikh, S. A., and Yau, G., "Seismic Behaviour of Concrete Columns Confined with Steel and Fiber-Reinforced Polymers," *ACI Structural Journal*, V. 99, No. 1, Jan.-Feb. 2002, pp. 72-80.

7. ACI Committee 318, 2002, "Building Code Requirements for Structural Concrete (ACI 318-02) and Commentary (318R-02)," American Concrete Institute, Farmington Hills, Mich., 443 pp.

8. Sheikh, S. A., and Khoury, S. S., "Confined Concrete Columns with Stubs," *ACI Structural Journal*, V. 90, No. 4, July-Aug. 1993, pp. 414-431.

9. Khoury, S. S., and Sheikh, S. A., "Behaviour of Normal and High Strength Confined Concrete Columns with and without Stubs," *Research Report* No. UHCEE 91-04, Department of Civil and Environmental Engineering, University of Houston, Tex., Dec. 1991, 345 pp.

10. "Code for Design of Concrete Structures (CSA Standard A23.3-94)," Canadian Standards Association, Rexdale, Ontario, Canada, 1994, 199 pp.

11. Bayrak, O., and Sheikh, S. A., "High-Strength Concrete Columns Under Simulated Earthquake Loading," *ACI Structural Journal*, V. 94, No. 6, Nov.-Dec. 1997, pp. 708-722.